








Endoplasmic reticulum stress and associated apoptosis are linked with the pathogenesis of white striping in broiler breast muscles

Emrah İpek,^{*} Umair Ahsan ^{†,‡} Bülent Özsoy [§], Gamze Sevri Ekren Aşıcı,^{||} Musa Tatar [#],
 Beyza Nur Özpilavcı,^{||} Erkmen Tuğrul Epikmen ^{*}, Şule Yurdagül Özsoy ^{*},
 Ehsan Karimiyan Khamseh [§], and Massimiliano Petracci ^{¶,1}

^{*}Department of Pathology, Faculty of Veterinary Medicine, Aydın Adnan Menderes University, Aydın 09016, Türkiye; [†]Department of Plant and Animal Production, Burdur Vocational School of Food, Agriculture and Livestock, Burdur Mehmet Akif Ersoy University, Burdur 15030, Türkiye; [‡]Center for Agriculture, Livestock and Food Research Burdur Mehmet Akif Ersoy University, Burdur 15030, Türkiye; [§]Department of Animal Nutrition and Nutritional Diseases, Faculty of Veterinary Medicine, Aydın Adnan Menderes University, Aydın 09016, Türkiye; ^{||}Department of Biochemistry, Faculty of Veterinary Medicine, Aydın Adnan Menderes University, Aydın 09016, Türkiye; [#]Department of Histology and Embryology, Faculty of Veterinary Medicine, Kastamonu University, Kastamonu, Türkiye; and [¶]Department of Agricultural and Food Sciences, Alma Mater Studiorum - University of Bologna, Bologna, Italy

ABSTRACT White striping (WS) that appears as white stripes parallel to the muscle fibrils is an emerging growth-related abnormality of broiler breast meat. The pathomechanism of this defect has not been fully understood despite intensive studies over the past decade. In the present study, endoplasmic reticulum (ER) stress and its associated apoptotic pathways were investigated to elucidate the potential role of these pathways in the development of WS. To this end, a total of 60 Pectoralis major (Pm) muscle samples were collected from 55-d-old Ross 308 male broiler chickens according to the severity of gross WS lesions (normal, mild, and severe). Histopathological and molecular analyses were conducted to evaluate the lesions and genes involved in the ER stress and related apoptosis. All the Pm samples, both with and without macroscopic WS lesions, showed varying degrees of myodegenerative lesions. Molecular analysis revealed that the

transcript abundances of many components related to protein kinase R-like ER kinase (PERK) and inositol-requiring enzyme type 1 (IRE-1) signals of the ER stress response were significantly greater in severely WS-affected breast tissues compared to their mildly affected and normal counterparts. Similarly, the transcript abundances of apoptotic markers related to both signaling pathways were significantly greater in severe WS lesions than those of mildly affected and normal Pm tissues. Besides these, a significant increase in *caspase-3* transcript abundance was seen in severe WS lesions in comparison with mild WS and normal breast muscles. Findings of this study suggest that ER stress response and its related apoptotic pathways are possibly activated in the breast muscle of broiler chickens with severe WS lesions. Based on these findings, it is speculated that ER stress-mediated apoptosis occupies a central role in the progression of WS in broiler chickens.

Key words: apoptosis, broiler chicken, endoplasmic reticulum stress, white striping

2024 Poultry Science 103:104103

<https://doi.org/10.1016/j.psj.2024.104103>

INTRODUCTION

Endoplasmic reticulum (ER) is a highly dynamic organelle consisting of anastomosed tubules and

flattened sacs that orchestrates the synthesis, folding, and maturation of cellular proteins. Proteins that gain entry into the ER lumen achieve their 3-dimensional structure there. Simultaneously, various post-translational modifications like glycosylation and formation of disulfide bonds are carried out by protein-folding and modification machinery (Berridge, 2002). Increased physiological requirements or pathological conditions such as hypoxia, calcium dysregulation, and others affect the ER folding capacity thereby initiating the accumulation of misfolded proteins in the ER lumen, a

© 2024 The Authors. Published by Elsevier Inc. on behalf of Poultry Science Association Inc. This is an open access article under the CC BY-NC-ND license (<http://creativecommons.org/licenses/by-nc-nd/4.0/>).

Received June 6, 2024.

Accepted July 11, 2024.

¹Corresponding author: m.petracci@unibo.it

phenomenon commonly referred to as ER stress. Several adaptation mechanisms known as “unfolded protein response” (UPR) are induced to reestablish the ER homeostasis to maintain cell survival (Hetz, 2012). Three sensor proteins namely double-stranded RNA-dependent protein kinase R (PKR)-like ER kinase (PERK), inositol-requiring protein 1 (IRE-1), and activating transcription factor 6 (ATF6), all located in the ER membrane carry out the UPR signaling cascade. This UPR response results in increased protein folding capacity, reduced protein synthesis, and stimulated degradation of misfolded proteins (Wang and Kaufman, 2016). However, any failure in the restoration of ER homeostasis turns the usual UPR signal into terminal UPR signal that triggers the apoptosis to eliminate the irreversibly damaged cells (Urrea et al., 2013).

Intensive breeding programs applied over the past decades to improve production traits in broiler chickens have significantly increased the incidence of growth-related abnormalities especially those affecting the Pectoralis major (Pm) muscle in fast-growing and heavy breast yielding hybrids (Barbut et al., 2024). White striping (WS) and wooden breast (WB) are among these pectoral muscle disorders characterized by distinctive phenotypes, however, exhibiting similar microscopic findings (Soglia et al., 2019). Although studies have suggested that the etiology of WS and WB is same, there is hardly any consensus on this issue (Soglia et al., 2021). Development of these defects has been associated with faster growth and high breast meat yield in modern broiler chicken hybrids (Kuttappan et al., 2013). These myopathies incur severe economic losses to poultry meat industry due to the deterioration of nutritional and technological qualities of breast meat (Barbut et al., 2024).

Several studies have been conducted to reveal the development mechanism of breast myopathies. Previous studies have suggested that the onset of breast myopathies in broiler chickens occurs in response to insufficiency of vasculature to support the fast-growing Pm muscle of modern broiler chickens (Kuttappan et al., 2013; Mutryn et al., 2015), thus developing the hypoxic condition that triggers the progression or increases the severity of these myopathies by reducing the oxygen supply (Soglia et al., 2019). Recent studies have emphasized that oxidative stress (Pampouille et al., 2019; Salles et al., 2019), mitochondrial dysfunction (Hosotani et al., 2020), and dysregulation of carbohydrate and lipid metabolism (Malila et al., 2019; Marchesi et al., 2019) contribute to the development of these defects. Besides these, other studies have suggested the involvement of ER stress and related UPR signaling in the pathogenesis of WB (Sihvo et al., 2017; Lake et al., 2019; Bordini et al., 2022; Greene et al., 2023) that offers a new strategy to prevent or suppress the development of breast myopathies in broiler chickens. Sihvo et al. (2017) described an increase in ER diameter of pectoral muscles affected with WB. Subsequent studies reported a difference in the expression of UPR-related genes in the Pm of WB-affected chickens (Lake et al., 2019; Bordini et al., 2022). Indeed, the protein synthesis upsurge

required to support the hypertrophic development of the Pm potentially overtaxes the capacity of the ER thus leading to the accumulation of misfolded and/or dysfunctional proteins such as collagen type IV (Bordini et al., 2024). Finally, hypoxia-induced activation of UPR and its related PERK-activating transcription factor 4 (ATF-4)-C/EBP homologous protein (CHOP) apoptotic pathway was demonstrated in WB-affected Pm muscle of broiler chickens (Greene et al., 2023). However, it is not known whether these mechanisms are involved in the pathogenesis of the pathological changes observed in WS as opposed to WB. Furthermore, apoptotic pathways induced by ER stress are not limited to PERK signaling only. Finally, once the process has been started, a time-series sequence of events begins thus resulting in the activation of complex response mechanisms (i.e., modifications in the energetic metabolism, inflammation, degeneration, and regeneration) which likely lead to the development of the growth-related defects such as WS (Barbut et al., 2024). Consequently, the pathomechanisms involved in the development of WS have not been fully elucidated yet. Therefore, potential role of ER stress and its induced apoptotic pathways in the development of WS were investigated for the first time in this study.

MATERIALS AND METHODS

The present study was conducted at Poultry Research Farm, Faculty of Veterinary Medicine, Aydın Adnan Menderes University, Türkiye pursuant to the prior approval of all the procedures in accordance with the guidelines of local animal care and use committee of the university vide letter number 64583101/2021/166.

Study Design, Animals, and Management Conditions

The study was conducted as a completely randomized design consisting of 3 groups based on the severity of WS on the breast muscles of broiler chickens as 1) normal (no WS lesion); 2) mild or low-grade WS lesion; and 3) severe or high-grade WS lesion.

A total of 60 one-d-old Ross 308 male broiler chickens weighing 44.0 ± 0.7 g on average, purchased from a local hatchery (Keskinoğlu Tavukçuluk ve Damızlık İşletmesi San. Tic. A.Ş. Manisa, Türkiye), were raised in deep litter system without grouping. Before the arrival of chickens, the house was thoroughly cleaned, nipple drinkers and feeders were installed, an 8 to 10 cm deep litter was spread, and heated to 33°C that was maintained in the first week. Temperature was gradually lowered by 3 to 3.5°C per week until 23°C which was maintained until the end of the rearing. Relative humidity was maintained between 50% and 70% throughout the rearing. A 20-h L: 4-h D lighting program was implemented in the first week followed by the application of 18-h L: 6-h D lighting program until the end of rearing. Broiler chickens were raised for 55 d comprising of 4 growth phases as

Table 1. Composition of diets used in starter (d 0–10), grower (d 11–24), finisher (d 25–39), and withdrawal (d 40–55) growth phases of broiler chickens.

Ingredients	Starter	Grower	Finisher	Withdrawal
Corn	53.810	59.337	60.883	64.974
Soybean meal	39.792	33.901	31.378	28.000
Sunflower oil	2.222	3.017	4.477	3.782
Dicalcium phosphate	1.780	1.545	1.323	1.284
Limestone	1.204	1.118	1.029	1.023
Common salt	0.327	0.326	0.326	0.325
DL-Methionine	0.296	0.200	0.176	0.140
L-Lysine HCl	0.224	0.229	0.138	0.182
L-Threonine	0.145	0.127	0.070	0.090
Vitamin premix ¹	0.100	0.100	0.100	0.100
Mineral premix ²	0.100	0.100	0.100	0.100
Chemical composition (% as fed basis)				
Crude protein	22.34	20.04	19.00	18.03
Metabolizable energy (kcal/kg)	3,000	3,100	3,200	3,200
Calcium	0.98	0.87	0.78	0.76
Total phosphorus	0.71	0.64	0.59	0.57
Available phosphorus	0.49	0.44	0.39	0.38
Digestible lysine	1.28	1.15	1.02	0.98
Digestible methionine	0.60	0.48	0.45	0.40
Digestible tryptophan	0.25	0.22	0.20	0.19
Digestible threonine	0.86	0.77	0.68	0.66
Digestible arginine	1.43	1.27	1.19	1.10
Digestible valine	0.96	0.87	0.82	0.78

¹Each kg contained: Vitamin A (as acetate) 12,000,000 IU; vitamin D₃ (as cholecalciferol) 5000,000 IU; vitamin E (as α -tocopherol acetate 50%) 100,000 mg; vitamin K₃ (as menadione sodium bisulphate 51 %) 4000 mg; vitamin B₁ (as thiamine mononitrate 98%) 3000 mg; vitamin B₂ (as riboflavin 80%) 8000 mg; niacin (as nicotinic amide 99%) 70,000 mg; vitamin B₅ (as calcium d-pantothenate 98%) 20,000 mg; vitamin B₆ (as proxidine hydrochloride 99%) 5,000 mg; vitamin B₁₂ (as cobalamin 1%) 30 mg; folic acid (91%) 2,000 mg; vitamin H₂ (as D-(+)-biotin 2%) 200 mg; calcium carbonate 63% (as carrier).

²Each kg contained: Manganese (as manganese oxide 62%) 150,000 mg; iron (as iron sulphate monohydrate 31%) 120,000 mg; zinc (as zinc oxide 72%) 120,000 mg; copper (as copper sulphate pentahydrate 25%) 12,000 mg; iodine (as calcium iodide 62%) 3000 mg; selenium (4.5%) 225 mg; molybdenum (as sodium molybdate 39%) 750 mg; calcium carbonate 13% (as carrier).

starter (d 0–10), grower (d 11–24), finisher (d 25–39), and withdrawal (d 40–55). Floor feeders were used during the starter phase and bell feeders were used from d 11 onwards. Ad libitum access to feed and water was provided throughout the rearing period. Diets used in the starter, grower, finisher, and withdrawal phases are presented in [Table 1](#).

Slaughtering Procedure and Sampling

At d 55, all the chickens were individually weighed, slaughtered by decapitation, feathers and skin were removed, abdomens were opened by dissection, and eviscerated. The Pm muscles were separated from the carcass and evaluated for WS lesions according to the visual scoring system previously described by [Kuttapan et al. \(2013\)](#) as normal (score 0; no striations), mild or moderate (score 1; <1 mm thick white striations), and severe (score 2; >1 mm thick white striations). Body weights of chickens were evaluated on the basis of WS lesion score. For histopathological examination, Pm muscle samples, each sizing 1 × 1 × 1 cm, were collected from the cranial one third of the right Pm muscle of all

chickens followed by immediate fixation for 24 to 48 h in neutral buffered formalin solution. Additionally, Pm muscle samples from each WS score (n = 12) were frozen in liquid nitrogen and stored at –80°C for PCR analysis.

Histopathological Examination

Following fixation, Pm samples were processed in an automatic tissue processor (TP1020, Leica Biosystems, IL) and paraffin blocks were prepared. Paraffin blocks were used to prepare 5 μ m thick tissue sections that were stained with hematoxylin-eosin (**HE**). Stained tissue sections were examined under a light microscope (BX51, Olympus, Tokyo, Japan) coupled with a digital camera (SC180, Olympus, Tokyo, Japan) and digital microscopic photographs were captured for histopathological evaluations.

Myodegeneration was scored using a 4-point scale adopted from [Prisco et al. \(2021\)](#). Accordingly, at least 10 different areas were evaluated at 20X magnification and scored as 0 = absence, 1 = mild (<10 myodegenerated fibrils); 2 = moderate (10 to 50% myodegenerated fibrils), and 3 = severe (>50% myodegenerated fibrils). Myodegenerated fibrils included swollen, rounded, loss of cross-striated architecture and hyalinized, and fragmented myofibrils invaded or surrounded by macrophages or heterophilic leukocytes. Occasionally, hyalinized myofibrils containing one or more vacuoles in their cytoplasm were assumed as myodegenerated. Perivenular lymphohistiocytic infiltration was evaluated according to the scoring system described by [Ahsan et al. \(2023\)](#). To this end, at least 10 areas were examined at 40X magnification to evaluate the average number of inflammatory cells per area by counting the number of inflammatory cells. Finally, the degree of inflammatory cell infiltration was scored on a 4-point scale as 0 = no infiltration, 1 = mild infiltration (5 to 25 inflammatory cells), 2 = moderate (26 to 50 inflammatory cells), and 3 = severe (>50 inflammatory cells). Replacement of adipose tissue or lipodosis was evaluated in accordance with the scoring method of [Prisco et al. \(2021\)](#). At least 10 fields were observed under 20X magnification and scored on a 4-point scale as 0 = no adipose tissue replacement, 1 = mild (<10% muscle fibers replaced), 2 = moderate (10 to 20% myofibers replaced), and 3 = severe (20% myofibers replaced). Besides these, collagen accumulation was evaluated in terms of presence or absence.

RNA Extraction and Quantitative RT-qPCR

Total RNA was extracted using an RNA isolation kit (Riboex, GeneAll Biotechnology, Seoul, Republic of Korea) according to the manufacturer's instructions followed by the measurement of RNA concentration and purity by spectrophotometry. A 2 μ g RNA was reverse transcribed using a cDNA synthesis kit (A.B.T. Laboratory Industry, Ankara, Türkiye). Then, the amplification was carried out by qPCR (StepOne Plus, Applied

Table 2. Primer sequences and GenBank accession number specific to the target genes.

Gene ¹	Accession number ²	Primer sequence	Orientation	Product size, bp
ATF4	NM_204880.3	TTGATGCCCTGTTAGGTATGGAA	Forward	138
		GTATGAGTGGAGGTTCTTTGTGT	Reverse	
GRP78	XM_046928788.1	CCCTCACCAAGGACAATCATC	Forward	240
		CCTCAGCAAACCTTCTCAGAC	Reverse	
NQO1	NM_001277619.2	GAGTGCTTTGTCTACGAGATGGA	Forward	104
		ATCAGGTCAGCCGCTTCAATC	Reverse	
XBP1	NM_001006192.2	CGAGTCTACGGATGTGAAGGAAT	Forward	139
		TGTGGAGGTTGTCAGGAATGG	Reverse	
EDEM1	NM_001006143.2	GGCTCATGACCTAGCAGTGAGA	Forward	62
		ACGGAATTCAGTTTTGGTGT	Reverse	
SEL1L	XM_040702156.2	GACTGGCATCAGAGCAACAG	Forward	160
		GCTAGGAAGACTGGAACCTGG	Reverse	
CHOP	XM_040693765.2	GCCGTGCTTAGCAGAATGG	Forward	92
		TGCTGTACAGTGGTGTGGAA	Reverse	
BIM	XM_025148907.3	AAGATCAGTGTTCCTGTGTAGAA	Forward	127
		GCTCCACTCTCCTTCCAATG	Reverse	
BAK1	NM_001030920.3	ATGGATGCCTGTCTGTCTGTTC	Forward	106
		GCAGAGCAGTCCAAAGACACTGA	Reverse	
BCL2	NM_205339.3	ATGACCGAGTACCTGAACCG	Forward	69
		CACAAAGCCATCCCATCCTC	Reverse	
Caspase 1	XM_015295935.4	CTTCCACGCCTGATACTGTC	Forward	183
		GCATTGTAGTCTCTCTTGTGT	Reverse	
Caspase 2	NM_001167701.2	TGGAAGAGATAAGCCTTTCTGAG	Forward	148
		TTAGAGAGCAGGATTTCTATTCCG	Reverse	
Caspase 3	NM_204725.2	CGGACTGTCTATCTCGTTCA	Forward	186
		TGGCTTAGCAACACACAAAAC	Reverse	
Caspase 8	NM_204592.4	TTCTGTAAACTAAATGGGAGCA	Forward	96
		GAGCAGACTGATGTCTTACTGAA	Reverse	
Caspase 9	XM_046903261.1	GGCTCCATCAGGGAATGAGG	Forward	179
		GGTCTTCAGAACGGGCGTAA	Reverse	
RPL30	NM_001007967.2	CTGTCTGCTTTGAGAAAATCG	Forward	161
		TGATGTCAGAGTCACTGGG	Reverse	

¹ATF4, activating transcription factor 4; GRP78, glucose-regulated protein 78; NQO1, NADPH quinone oxidoreductase 1; XBP1, X-box-binding protein 1; EDEM1, ER degradation enhancing Alpha-Mannosidase like protein 1; SEL1L, SEL1L ERAD E3 ligase adaptor subunit; CHOP, C/EBP homologous protein; BIM, BCL2 Like 11; BAK1, BCL2 antagonist/killer 1; BCL2, BCL2 apoptosis regulator; RPL30, ribosomal protein L30.

²Accession number refers to GenBank (NCBI) reference number.

Biosystems, Waltham, MA) using 2X qPCR Sybr-Green MasterMix (A.B.T. Laboratory Industry, Ankara, Türkiye). Specificity of the amplicons was checked by executing the melt curve analysis and agarose gel electrophoresis. Then, relative expression of the target genes was calculated using the $2^{-\Delta\Delta C_t}$ method (Livak and Schmittgen, 2001), with normalization to ribosomal protein L30 (RPL30) expression. Primer sequences specific to the target genes are listed in Table 2.

Statistical Analysis

Each broiler chicken served as an experimental unit for all the statistical evaluations. Normal distribution of data was tested with Shapiro–Wilk’s test and transformation of traits was carried out in case of non-normalized traits using logarithmic or square root transformation. Based on the type of data, parametric one-way analysis of variance or non-parametric Kruskal–Wallis tests were applied followed by Duncan’s multiple range test or Mann-Whitney U test with Bonferroni adjustment as post hoc, respectively. The differences among the means were assumed significant at 95% probability ($P < 0.05$). Results were presented as mean \pm standard error. Statistical analyses of the data were conducted using a computer-based statistical software package SPSS (version 22.0, IBM Corp., NY).

RESULTS

Gross Examination

The incidence of WS lesions was 73% (44/60) whereas, breast muscles of 16 out of 60 (27%) broiler chickens appeared normal (without WS lesions). Incidence of mild or moderate (score 1) WS lesions was 45% (27/60) whereas, that of severe (score 2) was 28% (17/60). Body weight of broiler chickens were not different among the WS scores (Figure 1).

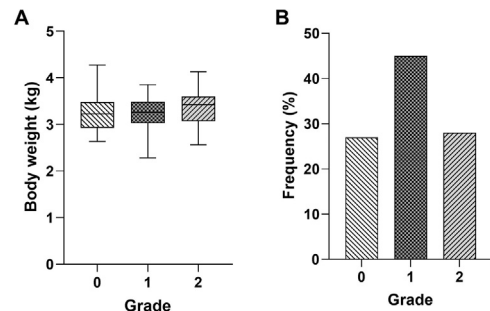


Figure 1. Body weight of broiler chickens (A) and gross lesion scores of white striping on Pectoralis major muscle (B). Breast muscles were macroscopically scored as grade 0 (normal), grade 1 (white striations <1mm thick), and grade 2 (white striations >1mm thick).

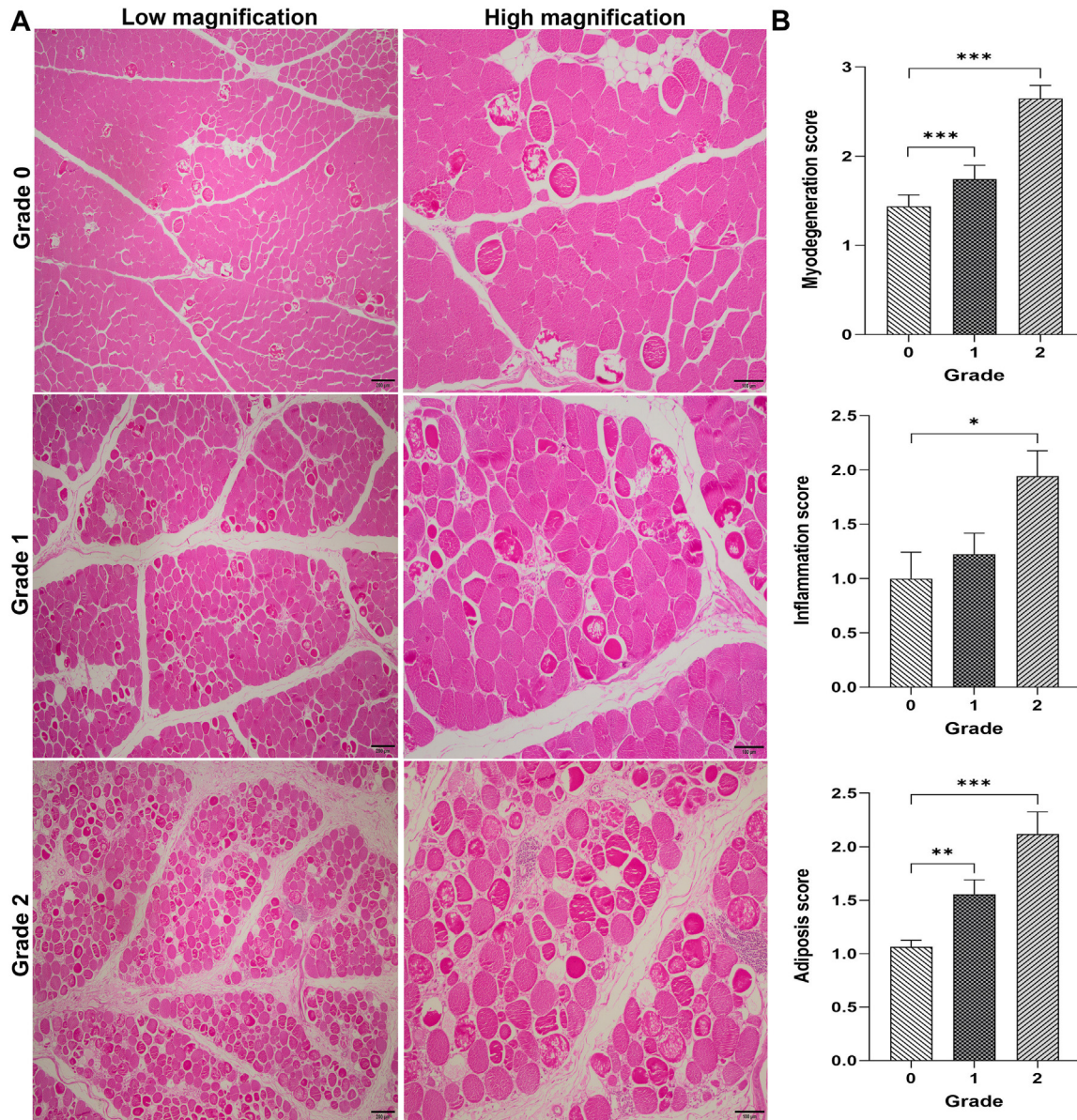


Figure 2. Microscopic findings. White striping myopathy, Pectoralis major muscle, chicken. Hematoxylin and eosin (HE). (A) Grade 0: some myodegenerative fibers (arrows) (<10% affected myofibrils) are present between the unaffected muscle fibers, Grade 1: moderate degeneration in muscle fibrils (10 to 50% of myofibrils affected), Grade 2: extensive degeneration in muscle fibrils (more than 50% of myofibrils affected). Interstitial areas seem expanded with loose fibrous tissue. Lymphohistiocytic inflammatory cell infiltrates can be seen around venules. Bars, 200 μm (for low magnifications) and 100 μm (for high magnifications). (B) Mean scores of histological lesions. Asterisk indicates statistical difference between macroscopic lesion scores (*: $P < 0.05$; **: $P < 0.01$; ***: $P < 0.001$).

Histopathology

Differences in myodegeneration, inflammation, and adiposis scores among the normal and WS-affected breast muscles of broiler chickens are shown in Figure 2.

Varying degrees of myodegenerative lesions were seen in all the examined breast muscles. Mild (9/16; 56%), moderate (6/16; 38%), and severe (1/16; 6%) myodegeneration was seen in Pm muscles scored as normal or without gross WS lesions. In Pm muscles with moderate WS lesions, myodegeneration was mild in 48% (13/27), moderate in 30% (6/27), and severe in 22% (6/27) of the samples. In severely WS-affected breast muscles, 6% (1/17) had mild, 24% (4/17) moderate, and 70% (12/17) had severe myodegenerative lesions. Myodegeneration score was greater in severely WS-affected Pm muscles

than their normal ($P < 0.001$) and moderately affected ($P < 0.001$) counterparts.

Perivascular lymphohistiocytic infiltration was mild in 31% (5/16), moderate in 25% (4/16), and severe in 6% (1/6) of normal breast muscles. Moderately WS-affected Pm muscles showed mild (8/27; 30%), moderate (8/27; 30%), and severe (3/27; 11%) perivascular infiltration. In Pm muscles with severe WS lesions, 26% (4/17) had mild, 29% (5/17) moderate, and 35% (6/17) had severe perivascular infiltration. Inflammation score was greater in severe WS group than normal breast muscle ($P < 0.05$).

In normal Pm muscles, lipidosis was mild in 94% (15/16) and moderate in 6% (1/16) samples. Lipidosis was mild in 44% (12/27), moderate in 44% (12/27), and severe in 7% (2/27) of moderately WS-affected Pm

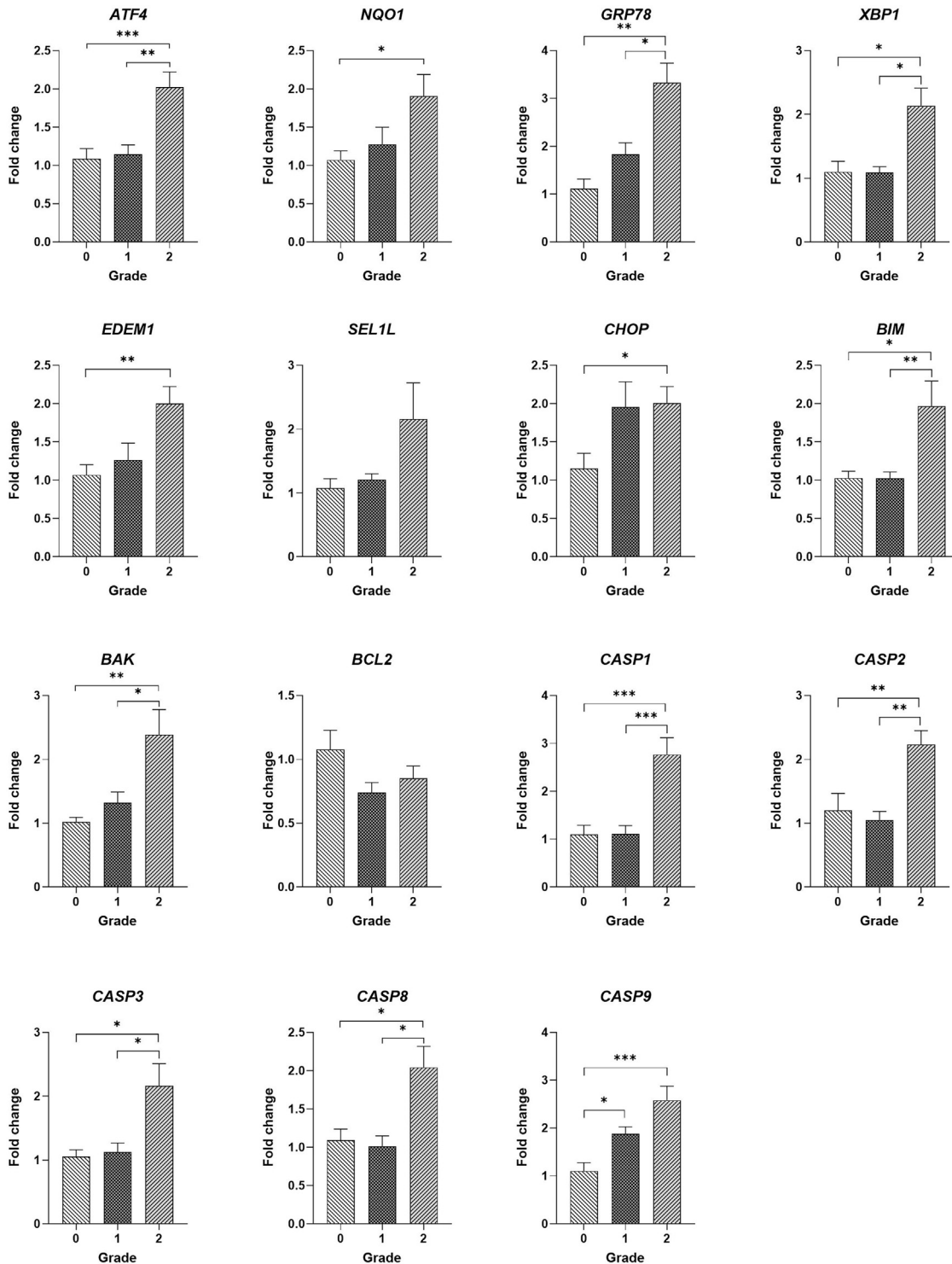


Figure 3. Findings of RT-qPCR. White striping myopathy, Pectoralis major muscle, chicken. The transcript abundances of ER stress and its related apoptotic markers. Relative abundance of the transcripts was analyzed by $2^{-\Delta\Delta C_t}$ method with RPL30 as a housekeeping gene. Asterisk indicates statistical difference between macroscopic lesion scores (*: $P < 0.05$; **: $P < 0.01$; ***: $P < 0.001$).

muscles. In Pm muscles with severe WS lesions, 12% (2/17) had mild, 47% (8/17) moderate, and 35% (6/17) had severe lipodosis. Lipodosis score was lower in normal breast muscle those having moderate ($P < 0.01$) and severe ($P < 0.001$) WS lesions.

Collagen accumulation between muscle bundles was seen in 13% (2/16) of normal, 33% (9/27) of moderately WS-affected, and 71% (12/17) of severely WS-affected breast muscles.

RT-qPCR

Figure 3 shows the transcript abundances of target genes measured using quantitative RT-qPCR. The transcript abundances of *ATF4*, glucose-regulated protein 78 (*GRP78*), and X-box binding protein 1 (*XBP1*) genes were greater in severe WS-affected Pm muscles than normal and moderately WS-affected breast muscles. Breast muscles with severe WS lesions had greater transcript

abundances of NADPH quinone oxidoreductase 1 (*NQO1*) and ER degradation enhancing alpha-mannosidase like protein 1 (*EDEM1*) compared to normal Pm muscles. The transcript abundances of SEL1L ERAD E3 ligase adaptor subunit (*SEL1L*) gene were not different among the breast muscle with or without WS lesions.

Breast muscles with severe WS lesions had greater transcript abundances of BCL2 like protein 11 (*BIM*), BCL2 antagonist/killer 1 (*BAK1*), *caspase 1*, *caspase 2*, *caspase 3*, and *caspase 8* genes than normal and moderately WS-affected Pm muscles. The transcript abundance of *caspase 9* gene was greater in breast muscle with WS lesions (both moderate and severe) than that of normal Pm muscles. In addition, the transcript abundance of *CHOP* gene was greater in Pm muscles with severe WS lesions than normal breast muscles. There was no difference in the transcript abundance of *BCL2* gene among the groups.

DISCUSSION

The present study witnesses the induction of ER stress in the Pm muscle of broiler chickens with severe WS. This study provides further evidence in relation to the activation of PERK and IRE1 arms of UPR signaling pathway to restore the ER homeostasis. However, apoptosis via PERK-ATF4-CHOP and IRE1-CASP2 and -CASP8 signals seems to have occurred in severely WS-affected Pm muscles of broiler chickens unable to cope with ER stress. Furthermore, pyroptosis is speculated to play a role in the stimulation of inflammatory response detected in the Pm muscles of chickens with myopathy.

Several studies have reported a dramatic increase in the incidence of WS exceeding 90% in recent years (Kuttappan et al., 2017; Malila et al., 2018; Prisco et al., 2021). In our study, the occurrence of WS was recorded at 73%, mostly as moderate WS lesions. Variations in incidence might be due to several intrinsic and extrinsic confounding factors including strain, age, sex, and diet (Kuttappan et al., 2016). Consistent with Prisco et al. (2021), histopathological lesions of varying degrees were seen in all broiler chickens examined with or without macroscopic WS lesions. This finding suggests that the incidence of WS is greater than reported. Generally, chickens without macroscopic lesions had mild histopathological lesions suggesting that these chickens may be in the early stages of the myopathy. As expected, varying degrees of polyphasic myodegeneration, perivascular lymphocytic infiltration, adipose tissue infiltration, and collagen accumulation between muscle bundles were seen in breast muscles of broiler chickens with WS (Kuttappan et al., 2017; Prisco et al., 2021; Ahsan et al. 2023).

Induction of UPR signal cascade in response to ER stress is controlled and driven by PERK, IRE1, and ATF6. These proteins monitor and perceive the protein folding conditions and initiate the signaling cascade through catalytic activities (Hetz and Papa, 2018). Activated PERK phosphorylates a subunit of eukaryotic

translation initiation factor 2α (**eIF2 α**) that reduces the overall translation initiation and protein synthesis in an attempt to decrease the protein load in ER (Walter and Ron, 2011). Additionally, p-eIF2 α selectively initiates the translation of a series of mRNAs such as ATF4 containing inhibitory upstream open reading frames in the 5' untranslated region (Harding et al., 2000a). In the present study, the transcript abundance of *ATF4* increased in Pm muscles of broiler chickens with severe WS compared to their normal or moderately affected counterparts indicating the potential activation of PERK signaling cascade in severely WS-affected breast muscles. Similar findings were reported by Greene et al. (2023) describing stimulated PERK signaling due to increase in PERK1 and p-eIF2 α levels in breast muscles with WB lesions. The onset of ER stress triggers the translocation of activated ATF4 to the nucleus that stimulates the expression of genes involved in protein folding, oxidative stress, and amino acid metabolism to reestablish ER homeostasis (Harding et al., 2003). Alongside an increase in *ATF4*, elevated transcript abundance of *GRP78* (responsible for protein folding) were detected in Pm muscles with severe WS lesions showing possibly enhanced protein folding capacity in severely WS-affected chickens to reduce ER stress. These data confirm the findings of previous studies (Kuttappan et al., 2017; Zhang et al., 2020).

Another downstream effector of activated PERK is the nuclear factor erythroid-related factor 2 (**NRF2**) that executes an important antioxidant response. Electron transport during disulfide bonds formation results in the production of reactive oxygen species in the ER lumen and PERK pathway activates an antioxidative response via phosphorylation of NRF2. Phosphorylated NRF2 translocates to the nucleus and triggers the transcription of antioxidant enzymes such as NQO1 (Zhang and Kaufman, 2008; Shelton and Jaiswal, 2013). In our study, there was a significant increase in the transcript abundance of *NQO1* in Pm muscles severe WS lesions in comparison with normal breast muscles. It can be speculated that a simultaneous increase in *NQO1* with *GRP78* might be due to the activation of antioxidant responses to limit the ROS formation due to excessive protein folding in broiler chickens with severe WS lesions.

The presence of unfolded protein in ER lumen causes dimerization of IRE1 that activates the kinase domain of IRE1. Auto- and transphosphorylation stimulate the endoribonuclease (**RNase**) activity of IRE1 (Gonzalez and Walter, 2001) that catalyzes the alternative splicing of mRNA encoding XBP1 thereby shifting the open reading sequence to form an active transcription factor XBP1s (Calfon et al., 2002). XBP1s translocates to the nucleus and triggers the transcription of genes involved in protein folding such as EDEM1, and those involved in the transport of proteins into the ER (Acosta-Alvear et al., 2007; Sicari et al., 2020). Increased transcript abundances of *XBP1* and its downstream effector molecule *EDEM1* in breast muscles with severe WS compared to normal Pm muscles suggest that in addition to PERK signaling the activation of IRE1 signal cascade might be

an attempt to cope with ER stress in WS-affected chickens. These data confirm the previous reports of [Welter et al. \(2022\)](#) and [Greene et al. \(2023\)](#) showing the activation of IRE1 signaling cascade in the breast muscle of chickens with growth-related myopathy.

ATF6, synthesized as an inactive precursor and activated in response to ER stress, is a transmembrane protein containing a transcription factor in cytosolic moiety. In the events of ER stress, it is transported from ER to Golgi body, processed by serine proteases, and a transcription factor ATF6f is released ([Haze et al., 1999](#)) and translocated to the nucleus to induce transcription of genes like *SEL1L* that regulate the ER homeostasis ([Asada et al., 2011](#)). In this study, transcript abundance of *SEL1L* in breast muscles was not different in chickens with or without WS myopathy suggesting that ATF6 arm of the UPR was not possibly induced in breast muscles of WS-affected broiler chickens.

Prolonged ER stress inflicts irreversible damage to the cells that are eliminated by apoptosis ([Urrea et al., 2013](#)). PCR analysis, in our study, revealed a considerable increase in the transcript abundance of *CASP3* in chickens with severe WS lesions on breast muscles compared to normal and moderate WS breast muscles. Our findings suggest that apoptosis might be induced in Pm muscles of chickens with severe WS. Consistent with these results, [Marchesi et al. \(2019\)](#) reported that genes related to the activation of apoptosis were differentially expressed revealed by whole transcriptomic analysis in WS-affected chickens. In this study, apoptotic pathways associated with ER stress in the WS-affected breast muscles of broiler chickens were investigated to evaluate whether ER stress stimulated the apoptosis, and if so, to explore the UPR arm involved in the apoptotic pathway.

Artificial sustained PERK activation has shown to stimulate the proliferation arrest and apoptosis ([Lin et al., 2009](#)). The major event mediating the transition from pro-survival response to pro-apoptotic response is the induction of CHOP by ATF4 ([Harding et al., 2000b](#)). In the present study, a substantial increase in the transcript abundance of *CHOP* in chickens with severe WS lesion than their normal counterparts. This suggests that the ability to overcome ER stress is seemingly impaired in severely WS-affected Pm muscles, thus directing the cells to apoptosis via PERK-ATF4-CHOP signaling pathway. These findings are consistent with those of [Greene et al. \(2023\)](#). Under the influence of ER stress, CHOP induces apoptosis by downregulating the expression of *BCL2* (a pro-survival proto-oncogene) and/or by upregulating the expression of pro-apoptotic BH3-only proteins such as *BIM* ([McCullough et al., 2001](#); [Lee et al., 2017](#)). BH3-only proteins act by inactivating *BCL2* to release *BAX* and *BAK* trapped by it, or by direct activation of *BAX* and *BAK*. Activated *BAX* and *BAK* serve to release the apoptotic molecules like cytochrome *c* via pore formation in the outer mitochondrial membrane. Cytochrome *c* binds with apoptotic peptidase activating factor 1 (**APAF1**) in cytosol to form apoptosome that serves as a platform for the activation of *CASP9*, which in turn, activates *CASP3*

leading to the induction of apoptosis ([Pihán et al., 2017](#)). In this study, broiler chickens with severe WS lesions had greater transcript abundances of *BIM*, *BAK1*, and *CASP9* than normal and moderately WS-affected chickens. Nonetheless, transcript abundance of *BCL2* was not different in broiler chickens with or without WS lesions. These findings indicate that CHOP-induced BH3-only proteins might have increased the mitochondrial permeability by stimulating *BAX* and *BAK*, which in turn triggered the apoptosis in chicken with severe WS myopathy.

Sustained ER stress increases RNase activity of IRE1 that decreases the specificity of IRE1 for *XBP1* as well as an increase in the degradation of specific class mRNAs, 28S ribosomal RNA, and microRNAs via a pathway namely regulated IRE1-dependent decay (**RIDD**). Degradation of RNA transcripts reduces the protein load in ER by declined mRNA translation. However, prolonged RIDD activity degrades anti-apoptotic microRNAs ([Maurel et al., 2014](#)) causing an increase in pro-apoptotic mediators like *CASP2* that drives apoptosis by enhancing the permeability of outer mitochondrial membrane through a *BID*-dependent pathway that stimulates apoptosis ([Upton et al., 2008; 2012](#)). Keeping this in view, we hypothesized that IRE1 signaling may contribute to the activation of apoptotic cell death detected in the breast muscle of WS-affected broiler chickens. As expected, the transcript abundance of *CASP2* was greater to a significant extent in chickens with severe WS than normal and moderately WS-affected chickens. Furthermore, hyperactivated IRE1 is known to trigger death receptor 5 (**DR5**) that contributes to the induction of apoptosis via a *CASP8* and *BID* mediated pathway ([Lu et al., 2014](#)). Considerably elevated transcript abundance of *CASP8* was witnessed in severely WS-affected chicken compared to those of normal and moderate WS thereby suggesting that these mediators possibly contribute to the induction of apoptosis via IRE1 in chickens with severe WS lesions.

Besides apoptosis, IRE1 signaling can induce pyroptosis by activating the inflammasome. Hyperactivation of IRE1 triggers pyroptosis via activation of an inflammatory caspase *CASP1* ([Lerner et al., 2012](#)). In our study, transcript abundance of *CASP1* was greater in chickens with severe WS than normal and moderate WS breast muscles. Previous studies have asserted the stimulation of inflammatory response and increase in pyroptosis-related cytokines like *IL-1 β* in chickens with growth-related breast myopathy ([Sihvo et al., 2017](#); [Xing et al., 2021](#)). Therefore, activation of *CASP1* via IRE1 signaling is speculated to induce an inflammatory response in the breast muscles of chickens with myopathy by possibly stimulating pyroptosis. Nevertheless, further studies are required to fully elucidate this mechanism.

CONCLUSIONS

To summarize, our findings demonstrate that activation of ER stress response and its related apoptotic

pathways are possibly linked with the pathogenesis of WS in the breast muscles of broiler chickens. Further investigations are required to elucidate the exact role of ER stress-mediated apoptosis in the development of WS.

ACKNOWLEDGMENTS

The authors gratefully acknowledge the financial support to this study by the Directorate of Scientific Research Projects (BAP), Aydın Adnan Menderes University, Türkiye wide project no. VTF-22005.

DISCLOSURES

The authors declare no conflicts of interest.

REFERENCES

- Acosta-Alvear, D., Y. Zhou, A. Blais, M. Tsikitis, N. H. Lents, C. Arias, C. J. Lennon, Y. Kluger, and B. D. Dynlacht. 2007. XBP1 controls diverse cell type- and condition-specific transcriptional regulatory networks. *Mol. Cell.* 27:53–66.
- Ahsan, U., E. İpek, Ö. S. Özdemir, A. K. Aydın, I. Raza, A. Çalık, E. Kuter, Ş. Y. Özsoy, and Ö. Cengiz. 2023. Intermittent dilution of dietary digestible lysine lowers the incidence of white striping by suppressing the growth, lipid synthesis, and muscle damage in broiler chickens. *J. Sci. Food Agric.* 103:283–297.
- Asada, R., S. Kanemoto, S. Kondo, A. Saito, and K. Imaizumi. 2011. The signalling from endoplasmic reticulum-resident bZIP transcription factors involved in diverse cellular physiology. *J. Biochem.* 149:507–518.
- Barbut, S., R. Mitchell, P. Hall, C. Bacon, R. Bailey, C. M. Owens, and M. Petracci. 2024. Review - myopathies in broilers: supply chain approach to provide solutions to challenges related to raising fast growing birds. *Poult. Sci.* 103:103801.
- Berridge, M. J. 2002. The endoplasmic reticulum: a multifunctional signaling organelle. *Cell Calcium* 32:235–249.
- Bordini, M., F. Soglia, R. Davoli, M. Zappaterra, M. Petracci, and A. Meluzzi. 2022. Molecular pathways and key genes associated with breast width and protein content in white striping and wooden breast chicken pectoral muscle. *Front. Physiol.* 13:936768.
- Bordini, M., M. Mazzoni, M. Di Nunzio, M. Zappaterra, F. Sirri, A. Meluzzi, M. Petracci, and F. Soglia. 2024. Time course evaluation of collagen type IV in Pectoralis major muscles of broiler chickens selected for different growth-rates. *Poult. Sci.* 103:103179.
- Calfon, M., H. Zeng, F. Urano, J. H. Till, S. R. Hubbard, H. P. Harding, S. G. Clark, and D. Ron. 2002. IRE1 couples endoplasmic reticulum load to secretory capacity by processing the XBP-1 mRNA. *Nature* 415:92–96.
- Gonzalez, T. N., and P. Walter. 2001. Ire1p: a kinase and site-specific endoribonuclease. *Methods Mol. Biol.* 160:25–36.
- Greene, E. S., C. Maynard, G. Mullenix, M. Bedford, and S. Dridi. 2023. Potential role of endoplasmic reticulum stress in broiler woody breast myopathy. *Am. J. Physiol. Cell Physiol.* 324: C679–C693.
- Harding, H. P., Y. Zhang, A. Bertolotti, H. Zeng, and D. Ron. 2000a. Perk is essential for translational regulation and cell survival during the unfolded protein response. *Mol. Cell.* 5:897–904.
- Harding, H. P., I. Novoa, Y. Zhang, H. Zeng, R. Wek, M. Schapira, and D. Ron. 2000b. Regulated translation initiation controls stress-induced gene expression in mammalian cells. *Mol. Cell.* 6:1099–1108.
- Harding, H. P., Y. Zhang, H. Zeng, I. Novoa, P. D. Lu, M. Calfon, N. Sadri, C. Yun, B. Popko, R. Paules, D. F. Stojdl, J. C. Bell, T. Hettmann, J. M. Leiden, and D. Ron. 2003. An integrated stress response regulates amino acid metabolism and resistance to oxidative stress. *Mol. Cell.* 11:619–633.
- Haze, K., H. Yoshida, H. Yanagi, T. Yura, and K. Mori. 1999. Mammalian transcription factor ATF6 is synthesized as a transmembrane protein and activated by proteolysis in response to endoplasmic reticulum stress. *Mol. Biol. Cell.* 10:3787–3799.
- Hetz, C. 2012. The unfolded protein response: controlling cell fate decisions under ER stress and beyond. *Nat. Rev. Mol. Cell Biol.* 13:89–102.
- Hetz, C., and F. R. Papa. 2018. The unfolded protein response and cell fate control. *Mol. Cell.* 69:169–181.
- Hosotani, M., T. Kawasaki, Y. Hasegawa, Y. Wakasa, M. Hoshino, N. Takahashi, H. Ueda, T. Takaya, T. Iwasaki, and T. Watanabe. 2020. Physiological and pathological mitochondrial clearance is related to pectoralis major muscle pathogenesis in broilers with wooden breast syndrome. *Front. Physiol.* 11:579.
- Kuttappan, V. A., H. L. Shivaprasad, D. P. Shaw, B. A. Valentine, B. M. Hargis, F. D. Clark, S. R. McKee, and C. M. Owens. 2013. Pathological changes associated with white striping in broiler breast muscles. *Poult. Sci.* 92:331–338.
- Kuttappan, V., B. Hargis, and C. Owens. 2016. White striping and woody breast myopathies in the modern poultry industry: a review. *Poult. Sci.* 95:2724–2733.
- Kuttappan, V. A., C. M. Owens, C. Coon, B. M. Hargis, and M. Vazquez-Añon. 2017. Incidence of broiler breast myopathies at 2 different ages and its impact on selected raw meat quality parameters. *Poult. Sci.* 96:3005–3009.
- Lake, J. A., M. B. Papah, and B. Abasht. 2019. Increased expression of lipid metabolism genes in early stages of wooden breast links myopathy of broilers to metabolic syndrome in humans. *Genes (Basel)* 10:746.
- Lee, S., S. Kim, S. Hwang, N. J. Cherrington, and D. Y. Ryu. 2017. Dysregulated expression of proteins associated with ER stress, autophagy and apoptosis in tissues from nonalcoholic fatty liver disease. *Oncotarget* 8:63370–63381.
- Lerner, A. G., J. P. Upton, P. V. Praveen, R. Ghosh, Y. Nakagawa, A. Igbaria, S. Shen, V. Nguyen, B. J. Backes, M. Heiman, N. Heintz, P. Greengard, S. Hui, Q. Tang, A. Trusina, S. A. Oakes, and F. R. Papa. 2012. IRE1 α induces thioredoxin-interacting protein to activate the NLRP3 inflammasome and promote programmed cell death under irremediable ER stress. *Cell Metab* 16:250–264.
- Lin, J. H., H. Li, Y. Zhang, D. Ron, and P. Walter. 2009. Divergent effects of PERK and IRE1 signaling on cell viability. *PLoS One* 4: e4170.
- Livak, K. J., and T. D. Schmittgen. 2001. Analysis of relative gene expression data using real-time quantitative PCR and the 2(-Delta Delta C(T)) Method. *Methods* 25:402–408.
- Lu, M., D. A. Lawrence, S. Marsters, D. Acosta-Alvear, P. Kimmig, A. S. Mendez, A. W. Paton, J. C. Paton, P. Walter, and A. Ashkenazi. 2014. Opposing unfolded-protein-response signals converge on death receptor 5 to control apoptosis. *Science* 345:98–101.
- Malila, Y., J. U-Chupaj, Y. Srimarut, P. Chaiwiwatrakul, T. Uengwetwanit, S. Arayamethakorn, V. Punyapornwithaya, C. Sansamur, C. P. Kirschke, L. Huang, S. Tepasamorndech, M. Petracci, W. Rungrasamee, and W. Visessanguan. 2018. Monitoring of white striping and wooden breast cases and impacts on quality of breast meat collected from commercial broilers (*Gallus gallus*). *Asian-Australas. J. Anim. Sci.* 31:1807–1817.
- Malila, Y., K. Thanatsang, S. Arayamethakorn, T. Uengwetwanit, Y. Srimarut, M. Petracci, G. M. Strasburg, W. Rungrasamee, and W. Visessanguan. 2019. Absolute expressions of hypoxia-inducible factor-1 alpha (HIF1A) transcript and the associated genes in chicken skeletal muscle with white striping and wooden breast myopathies. *PLoS One* 14:e0220904.
- Marchesi, J. A. P., A. M. G. Ibelli, J. O. Peixoto, M. E. Cantão, J. R. C. Pandolfi, C. M. M. Marciano, R. Zanella, M. L. Settles, L. L. Coutinho, and M. C. Ledur. 2019. Whole transcriptome analysis of the pectoralis major muscle reveals molecular mechanisms involved with white striping in broiler chickens. *Poult. Sci.* 98:590–601.
- Maurel, M., E. Chevet, J. Tavernier, and S. Gerlo. 2014. Getting RIDD of RNA: IRE1 in cell fate regulation. *Trends Biochem. Sci.* 39:245–254.
- McCullough, K. D., J. L. Martindale, L. O. Klotz, T. Y. Aw, and N. J. Holbrook. 2001. Gadd153 sensitizes cells to endoplasmic

- reticulum stress by down-regulating Bcl2 and perturbing the cellular redox state. *Mol. Cell Biol.* 21:1249–1259.
- Mutryn, M. F., E. M. Brannick, W. Fu, W. R. Lee, and B. Abasht. 2015. Characterization of a novel chicken muscle disorder through differential gene expression and pathway analysis using RNA-sequencing. *BMC Genomics* 16:399.
- Pampouille, E., C. Hennequet-Antier, C. Praud, A. Juanchich, A. Brionne, E. Godet, T. Bordeau, F. Fagnoul, E. Le Bihan-Duval, and C. Berri. 2019. Differential expression and co-expression gene network analyses reveal molecular mechanisms and candidate biomarkers involved in breast muscle myopathies in chicken. *Sci. Rep.* 9:14905.
- Pihán, P., A. Carreras-Sureda, and C. Hetz. 2017. BCL-2 family: integrating stress responses at the ER to control cell demise. *Cell Death Differ* 24:1478–1487.
- Prisco, F., D. De Biase, G. Piegari, I. d’Aquino, A. Lama, F. Comella, R. Mercogliano, L. Dipineto, S. Papparella, and O. Paciello. 2021. Pathologic characterization of white striping myopathy in broiler chickens. *Poult. Sci.* 100:101150.
- Salles, G. B. C., M. M. Boiago, A. D. Silva, V. M. Morsch, A. Gris, R. E. Mendes, M. D. Baldissera, and A. S. da Silva. 2019. Lipid peroxidation and protein oxidation in broiler breast fillets with white striping myopathy. *J. Food Biochem.* 43:e12792.
- Shelton, P., and A. K. Jaiswal. 2013. The transcription factor NF-E2-related factor 2 (Nrf2): a protooncogene? *FASEB J* 27:414–423.
- Sicari, D., A. Delaunay-Moisan, L. Combettes, E. Chevet, and A. Igbaria. 2020. A guide to assessing endoplasmic reticulum homeostasis and stress in mammalian systems. *FEBS J* 287:27–42.
- Sihvo, H. K., J. Lindén, N. Airas, K. Immonen, J. Valaja, and E. Puolanne. 2017. Wooden breast myodegeneration of pectoralis major muscle over the growth period in broilers. *Vet. Pathol.* 54:119–128.
- Soglia, F., M. Mazzoni, and M. Petracci. 2019. Spotlight on avian pathology: current growth-related breast meat abnormalities in broilers. *Avian Pathol* 48:1–3.
- Soglia, F., M. Petracci, R. Davoli, and M. Zappaterra. 2021. A critical review of the mechanisms involved in the occurrence of growth-related abnormalities affecting broiler chicken breast muscles. *Poult. Sci.* 100:101180.
- Upton, J. P., L. Wang, D. Han, E. S. Wang, N. E. Huskey, L. Lim, M. Truitt, M. T. McManus, D. Ruggero, A. Goga, F. R. Papa, and S. A. Oakes. 2012. IRE1 α cleaves select microRNAs during ER stress to derepress translation of proapoptotic Caspase-2. *Science* 338:818–822.
- Upton, J. P., K. Austgen, M. Nishino, K. M. Coakley, A. Hagen, D. Han, F. R. Papa, and S. A. Oakes. 2008. Caspase-2 cleavage of BID is a critical apoptotic signal downstream of endoplasmic reticulum stress. *Mol. Cell Biol.* 28:3943–3951.
- Urra, H., E. Dufey, F. Lisbona, D. Rojas-Rivera, and C. Hetz. 2013. When ER stress reaches a dead end. *Biochim. Biophys. Acta.* 1833:3507–3517.
- Walter, P., and D. Ron. 2011. The unfolded protein response: from stress pathway to homeostatic regulation. *Science* 334:1081–1086.
- Wang, M., and R. J. Kaufman. 2016. Protein misfolding in the endoplasmic reticulum as a conduit to human disease. *Nature* 529:326–335.
- Welter, A. A., W. J. Wu, R. Maurer, T. G. O’Quinn, M. D. Chao, D. L. Boyle, E. R. Geisbrecht, S. D. Hartson, B. C. Bowker, and H. Zhuang. 2022. An investigation of the altered textural property in woody breast myopathy using an integrative omics approach. *Front. Physiol.* 13:860868.
- Xing, T., D. Luo, X. Zhao, X. Xu, J. Li, L. Zhang, and F. Gao. 2021. Enhanced cytokine expression and upregulation of inflammatory signaling pathways in broiler chickens affected by wooden breast myopathy. *J. Sci. Food Agric.* 101:279–286.
- Zhang, K., and R. J. Kaufman. 2008. From endoplasmic-reticulum stress to the inflammatory response. *Nature* 454:455–462.
- Zhang, X., D. Antonelo, J. Hendrix, V. To, Y. Campbell, M. Von Staden, S. Li, S. P. Suman, W. Zhai, J. Chen, H. Zhu, and W. Schilling. 2020. Proteomic characterization of normal and woody breast meat from broilers of five genetic strains. *Meat Muscle Biol* 4:9